

## Measurements of the Deuterium-Tritium Branching Ratio Using ICF Implosions

Y. Kim 1), H.W. Herrmann 1), J.M. Mack 1), C.S. Young 1), J.R. Langenbrunner 1), S. Evans 1), T. Sedillo 1), A.M. McEvoy 1), C.J. Horsfield 2), M. Rubery 2), Z. Ali 3), and W. Stoeffl 4)

1) Los Alamos National Laboratory, Los Alamos, NM 87545, USA

2) Atomic Weapons Establishment, Aldermaston, Reading, RG7 4PR, UK

3) National Security Technologies, Livermore, CA 94550, USA

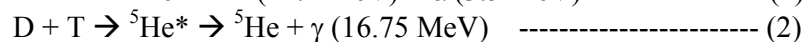
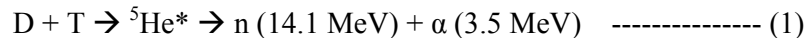
4) Lawrence Livermore National Laboratory, Livermore, CA 94550, USA

E-mail contact of main author: yhkim@lanl.gov

**Abstract.** A neutron-induced gamma experiment was carried out using a Gas Cherenkov Detector (GCD) at the OMEGA laser facility. The high-bandwidth of the GCD allows for the detection of DT fusion gamma rays before the 14.1 MeV neutrons arrive at the GCD, relieving the measurement of undesired neutron background. Absolute DT fusion gamma-ray signal has been determined by various secondary target materials such as Si, SiO<sub>2</sub>, Al, Al<sub>2</sub>O<sub>3</sub>, or Cu which were placed near target chamber center (TCC). 14.1 MeV neutrons interact with the secondary targets and produce neutron-induced gamma-rays, which are used to calibrate the GCD. In conjunction with an independent neutron yield measurement and a coupled MCNP/ACCEPT simulation code, the resultant DT branching ratio was inferred.

### 1. Introduction

Fusion of deuterium (D) and tritium (T) produces an excited <sup>5</sup>He\* nucleus, which has several possible de-excitation modes. The most common mode results in the emission of a 14.1 MeV neutron and a 3.5 MeV alpha particle. A much less frequent mode involves the excited <sup>5</sup>He\* nucleus relaxing to the ground state via the emission of a 16.75 MeV gamma ray [1].



Historically, interest has been focused on the measurement of reaction yield ratio for reaction (2) relative to reaction (1), which is the DT branching ratio:  $BR_{\gamma/n}^{DT} = \frac{T(D,\gamma)}{T(D,n)}$ .

Experimental branching ratio values reported prior to 1984 are disparate by a factor of 30. Branching ratio values reported since 1984 vary from  $5 \times 10^{-5}$  to  $1 \times 10^{-4}$ . All existing measurements have been accelerator-based (> 100 keV) and compromised by target design difficulties and intractable 14.1 MeV neutron-induced radiation backgrounds.

Recent advances in Cherenkov diagnostics and Monte Carlo simulations developed at Los Alamos National Laboratory (LANL) have allowed for more precise DT branching ratio measurements at ICF (Inertial Confinement Fusion) implosion. The high-bandwidth of the Gas Cherenkov Detector (GCD) allows for the detection of DT fusion gamma rays before the 14.1 MeV neutrons arrive at the GCD, relieving the measurement of undesired neutron background [2].

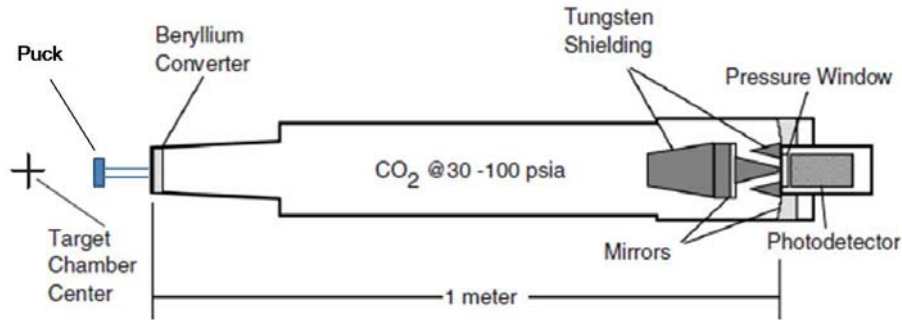


FIG. 1. Schematic diagram of GCD and secondary neutron-induced gamma-ray target. Secondary target is used to calibrate the efficiency of GCD.

Absolute DT fusion gamma-ray signal has been determined by various secondary target materials such as Si, SiO<sub>2</sub>, Al, Al<sub>2</sub>O<sub>3</sub>, or Cu which were placed near target chamber center (TCC). 14.1 MeV neutrons interact with the secondary targets and produce neutron-induced gamma-rays, which are used to calibrate the GCD. In conjunction with an independent neutron yield measurement and a coupled MCNP/ACCEPT simulation code, the resultant DT branching ratio was inferred.

## 2. Experimental Methods

Figure 1 shows schematic of the GCD and associated secondary gamma-ray target. The GCD used for these studies is described in greater detail elsewhere [2]. Briefly, fusion gammas are converted to relativistic electrons primarily through Compton scattering and pair production in a beryllium converter on the front of the detector. Electrons traveling faster than the speed of light in the gas then produce Cherenkov radiation as they travel through a pressurized CO<sub>2</sub> gas cell. The pressure of CO<sub>2</sub> in the gas cell determines the index of refraction and thus speed of light in the medium, hence establishing a variable energy thresholding capability. This UV/visible light is then collected onto an ultra-fast PMT and the signal is recorded on high bandwidth recorders.

Secondary targets, otherwise called pucks, were placed between TCC and GCD at a distance  $L_p = 58$  mm (or 56.65 mm, depending on the type of puck). The pucks had a diameter  $D_p = 30$  mm (or 25.4 mm), and a thickness  $T_p = 5$  mm (or 6.35 mm). A puck holder made of Aluminum was used to hold a puck and attached to the nose cone of the GCD. The GCD nose cone was located 20 cm away from TCC.

## 3. Experimental Results

Figure 2a shows time-dependent gamma-ray signals from DT-filled plastic capsule implosions. The black curve was obtained without a puck inserted to serve as a baseline while the red curve was measured with a Si puck in place. 60 laser beams were used with a total energy of 23 kJ of UV light on target. Silicon puck ( $D = 25.4$  mm,  $t = 6.35$  mm) was placed 5.665 cm away from TCC for shot 54453. The CO<sub>2</sub> gas pressure in the GCD was fixed at 100 psia, which corresponds to a threshold energy ( $E_{th}$ ) of  $\sim 6.3$  MeV. Both  $\gamma$ -signals are normalized by neutron-yield and a MCP gain value of 521. Time zero is placed at the highest peak of signals (peak B) for convenience.

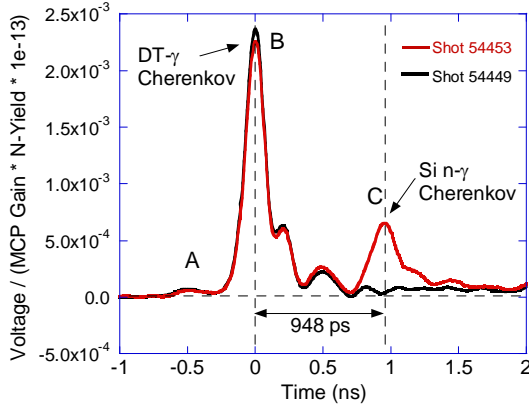


FIG. 2a. Simultaneous measurement of fusion gamma and secondary Si gamma signals

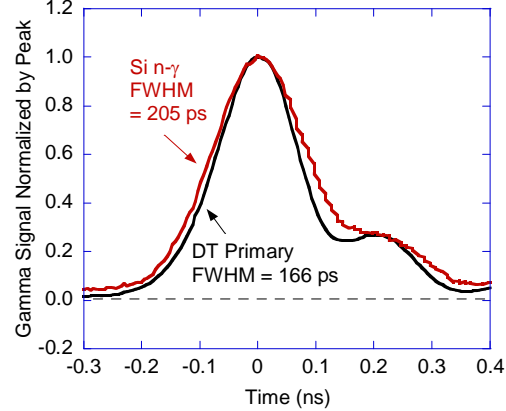


FIG. 2b. DT branching ratio derived from secondary n-gamma experiment

Without puck (black curve), reproducible DT- $\gamma$  signals are measured and served as baseline for n- $\gamma$  study. As explained in ref 2, a precursor (peak A) and a DT- $\gamma$  (peak B) are detected. With puck (red curve), new signal peak (peak C) was observed at the 948 ps later. The time interval measured between peaks B and C (= 948 ps) is quite consistent with the expected time-of-flight difference between DT- $\gamma$  and 14 MeV neutrons ( $\sim 163$  ps/cm) incident on the Si puck (=  $163$  ps/cm  $\times 5.665$  cm =  $923$  ps). Si n- $\gamma$  signal shape was compared with that of DT- $\gamma$  by normalizing each peaks (B and C) with their own peak height and overlaying peak C and B. Shown in Fig. 2b, full-width half maximum (FWHM) of the Si n- $\gamma$  signal was 205 ps, which is wider than that of DT- $\gamma$  signal (166 ps). The measured Si n- $\gamma$  FWHM was quite close to the estimated value ( $\sim 207$  ps =  $(166^2 + 16^2 + 123^2)^{1/2}$  ps) by taking account of 1) measured DT- $\gamma$  FWHM (= 166 ps), 2) neutron Doppler broadening time ( $\sim 16$  ps at 5.665 cm) and 3) geometrical temporal spreading as the neutrons penetrate the puck ( $\sim 123$  ps). High-band width of the GCD enabled us to detect time delayed and Doppler broadened n- $\gamma$  signals from the puck.

Four more puck materials ( $\text{SiO}_2$ ,  $\text{Al}_2\text{O}_3$ , Al, and Cu) were tested with  $E_{\text{th}}$  kept at 6.3 MeV. Two shots were carried out for each puck. Each n- $\gamma$  signal is normalized by corresponding neutron-yield and MCP gain. The baseline-subtracted n- $\gamma$  signals are overlaid and shown in the vicinity of peak C in Figure 3. The silicon puck produced the strongest secondary signal ratioed to the DT- $\gamma$  signal (n- $\gamma$ /DT- $\gamma \sim 27\%$ ). The n- $\gamma$ /DT- $\gamma$  of  $\text{SiO}_2$  and  $\text{Al}_2\text{O}_3$  were similar at  $\sim 12\%$ . The n- $\gamma$ /DT- $\gamma$  of Al was  $\sim 9\%$ . Copper produced the weakest n- $\gamma$  above 6.3 MeV at n- $\gamma$ /DT- $\gamma \sim 7\%$ . Measured n- $\gamma$  signals for the five puck materials are used as simulation codes validation purpose such as a MCNP (Monte Carlo N-Particle) code for n- $\gamma$  production and an ITS ACCEPT code for GCD spectral sensitivity.

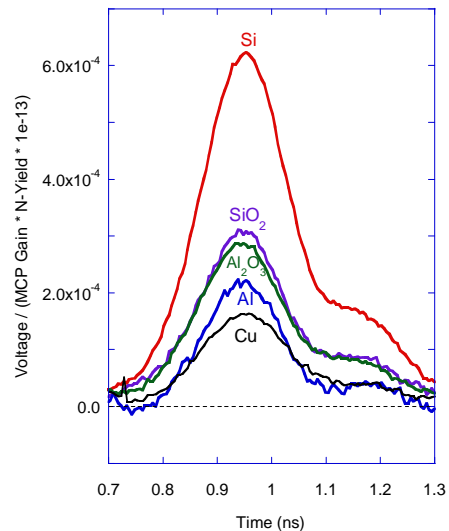


FIG. 3. n- $\gamma$  material sensitivity measured by GCD.

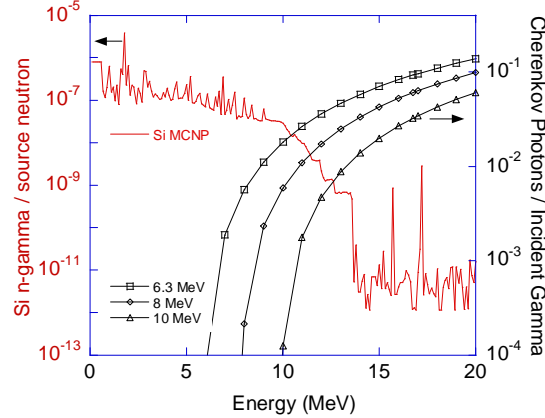


FIG. 4. Si n- $\gamma$  spectrum simulated by MCNP (red curve) and GCD sensitivity as a function of threshold energy (black curves).

#### 4. Data Analysis

The GCD sensitivity to n- $\gamma$  was simulated using MCNP for the Si n- $\gamma$  spectrum (red curve in Fig. 4) and using ITS ACCEPT for the GCD responses to various  $\gamma$ -ray energies (black curve in Fig. 4) for varying  $E_{th}$ . Secondary n- $\gamma$  spectrum decreases as energy increases, with little n- $\gamma$  occurring above 10 MeV. Therefore, secondary gammas can be thresholded out by increasing  $E_{th}$ , while the sensitivity to DT- $\gamma$  at 16.75 MeV is only marginally reduced.

Table I shows the branching ratio values derived from different puck n- $\gamma$  experiment. In conjunction with an independent neutron yield measurement and a coupled MCNP/ACCEPT simulation code, the detection efficiency of the GCD has been estimated from the n- $\gamma$  measurement. In other word, secondary targets served as in-situ GCD detector calibration sources. Finally, the absolute DT fusion gamma-ray signal (peak B) has been determined and resultant DT  $\gamma$ /n branching ratio is inferred. We report a preliminary measurement of the DT branching ratio of  $(3.3 \pm 1.4) \times 10^{-5}$  as measured at ICF implosions.

Table I: DT branching ratio inferred with various neutron target materials

	Measured n- $\gamma$ (Coulombs)	Measured DT- $\gamma$ (Coulombs)	n- $\gamma$ /DT- $\gamma$ (%)	Calculated n- $\gamma$ (# photon/neutron)	Calculated DT- $\gamma$ (# photon/ $\gamma$ )	Branching Ratio
Si	1.55e-12	5.26e-12	29.5	8.17e-9	1.13e-3	2.47e-5
SiO2	6.86e-13	5.26e-12	13.0	6.16e-9	1.13e-3	4.18e-5
Al	5.89e-13	5.91e-12	11.2	4.98e-9	1.13e-3	4.42e-5
Al2O3	5.99e-13	5.26e-12	11.4	7.14e-9	1.13e-3	5.55e-5
Cu	3.90e-13	5.26e-12	7.4	1.81e-9	1.13e-3	2.16e-5

#### 5. Conclusion

A neutron-induced gamma experiment was carried out using a Gas Cherenkov Detector (GCD) at the OMEGA laser facility. The high-bandwidth of the GCD allows for the detection of DT fusion gamma rays before the 14.1 MeV neutrons arrive at the GCD, relieving the measurement of undesired neutron background. Absolute DT fusion gamma-ray signal has

been determined by various secondary target materials such as Si, SiO<sub>2</sub>, Al, Al<sub>2</sub>O<sub>3</sub>, or Cu which were placed near target chamber center (TCC). 14.1 MeV neutrons interact with the secondary targets and produce neutron-induced gamma-rays, which are used to calibrate the GCD. In conjunction with an independent neutron yield measurement and a coupled MCNP/ACCEPT simulation code, the resultant DT branching ratio was inferred. We report a preliminary measurement of the DT branching ratio of  $(3.3 \pm 1.4) \times 10^{-5}$  as measured at ICF implosions. Improved measurements of the DT branching ratio are beneficial to gamma-ray-based DT burn-history measurements for the National Ignition Facility (NIF) and other facilities contemplating the need for similar diagnostic information.

### References

- [1] MACK, J.M., et al., "Remarks on detecting high-energy deuterium-tritium fusion gamma rays using a gas Cherenkov detector", *Rad. Phys. Chem.* **75** (2006) 551
- [2] HERRMANN H.W., et al., "Cherenkov radiation conversion and collection considerations for a gamma bang time/reaction history diagnostic for the NIF", *Rev. Sci. Instrument* **79** (2008) 10E531